Journal of Testing and Evaluation

Ning Fang[1] and P. Srinivasa Pai[2]

DOI: 10.1520/JTE20180279

Evaluation and Modeling of the Effect of Tool Edge Radius on Machined Surface Roughness in Turning UNS A92024-T351 Aluminum Alloy

Journal of Testing and Evaluation

doi:10.1520/JTE20180279 available online at www.astm.org

Ning Fang[1] and P. Srinivasa Pai[2]

Evaluation and Modeling of the Effect of Tool Edge Radius on Machined Surface Roughness in Turning UNS A92024-T351 Aluminum Alloy

Reference

N. Fang and P. Srinivasa Pai, "Evaluation and Modeling of the Effect of Tool Edge Radius on Machined Surface Roughness in Turning UNS A92024-T351 Aluminum Alloy," *Journal of Testing and Evaluation* https://doi.org/10.1520/JTE20180279

ABSTRACT

Tool edge radius plays a significant role in affecting the surface integrity of machined products. The vast majority of existing research, however, takes no account of the effect of tool edge radius in the evaluation and modeling of machined surface roughness, an essential indicator of surface integrity. The present study fills this important research gap and has performed a total of 45 turning experiments on Unified Numbering System (UNS) A92024-T351 aluminum alloy with carefully selected cutting tools with three levels of tool edge radii. This article describes the experimental setup and measurements of tool edge radius and machined surface roughness. Machined surface roughness was evaluated using five parameters, including average roughness, root-mean-square roughness, peak roughness, maximum roughness height, and five-point average roughness. The experimental evidence presented in this article shows that the tool edge radius has a profound effect on machined surface roughness, cutting forces, and cutting vibrations. Based on the experimental data, three types of predictive models are developed, including a multiple regression model, multilayer perceptron neural network model, and radial basis function neural network model. The prediction accuracy of the three models is compared based on average mean squared errors. The results show that different models lead to different prediction accuracy for different surface roughness parameters.

Keywords

tool edge radius, machined surface roughness, evaluation, modeling, cutting forces, cutting vibrations

Manuscript received April 19, 2018; accepted for publication December 21, 2018; published online March 18, 2019.

[1] College of Engineering, Utah State University, 4160 Old Main Hill, Logan, UT 84322-4160, USA (Corresponding author), e-mail: ning.fang@usu.edu, https://orcid.org/0000-0002-9380-3608

[2] College of Engineering, Utah State University, 4160 Old Main Hill, Logan, UT 84322-4160, USA

Nomenclature

f = Feed rate
F_c = Cutting force
F_f = Feed force
F_p = Passive force
R_a = Average roughness
R_{max} = Maximum roughness height
R_p = Peak roughness
R_q = Root-mean-square roughness
R_z = Five-point average roughness
r = Ratio of feed rate to tool edge radius
V = Cutting speed
V_x = Cutting vibration in the cutting speed direction
V_y = Cutting vibration in the feed rate direction
V_z = Cutting vibration in the depth of cut direction
r_e = Tool edge radius

Introduction

THE IMPORTANT EFFECT OF TOOL EDGE RADIUS IN MACHINING

Machining is a material removal process widely employed in modern manufacturing. The quality of machined products, such as the dimensional accuracy and surface integrity, depends on many factors, for example tool geometry, work material, and cutting conditions employed in machining. Tool geometry typically includes tool rake angle, tool flank angle, tool inclination angle, tool nose radius (also called tool corner radius), tool edge radius, and so on. Recent years have seen a growing interest in and need to incorporate the effect of tool edge radius in the predictive modeling of machining because of the rapid development and application of precision and ultraprecision machining in a variety of modern industries, such as the aerospace, automotive, and die- and mold-making industries.

In precision and ultraprecision machining, the feed rate is often in the same magnitude as the tool edge radius. The effect of the tool edge radius cannot be neglected because extensive experimental evidence has suggested that the tool edge radius significantly affects chip formation,[1–3] cutting forces,[4–6] cutting temperatures,[7] tool wear,[8] and surface integrity.[9] For example, Arif, Rahman, and San[5] found that tool edge radius affects crack propagation in the cutting zone in the ductile-mode machining of brittle materials, such as tungsten carbides. Nasr, Ng, and Elbestawi[9] developed an Arbitrary Lagrangian-Eulerian finite element model to simulate the effect of tool edge radius on the residual stress of machined surfaces in orthogonal cutting. They found that a larger tool edge radius induced higher residual stress in both the tensile and compressive regions of the machined surface.

MACHINED SURFACE ROUGHNESS

The surface roughness of machined products, or simply machined surface roughness, is a widely used index of product quality because it significantly affects the surface integrity, dimensional accuracy, wear resistance, and fatigue strength of machined products.[10–12] Research has been conducted to study factors affecting machined surface roughness[13,14] and develop various methods for surface roughness evaluation.[15–17]

For example, Grum and Kisin[14] conducted turning experiments on three two-phase alloys (aluminum silicon [AlSi] 5, AlSi2, and AlSi20) with different soft-phase sizes. They concluded that material microstructure also plays an important role in affecting average surface roughness. Scandiffio, Diniz, and de Souza[15] studied machined surface roughness, tool life, and machining force in milling free-form shaped, hardened AISI D6 steel with

cemented carbide tools. They found that the average surface roughness varied in descendant and ascendant milling conditions and was affected by the combined effect of machining forces and vibrations.

The evaluation and modeling of machined surface roughness is important for machining process planning and optimization, such as the optimal design and selection of tool geometry and cutting conditions. In an effort to correlate cutting conditions with cutting forces and machined surface roughness in end milling, Maher et al.[18] developed an adaptive neuro-fuzzy inference system model to predict average surface roughness using cutting force data. Wang et al.[19] performed lens slow tool servo turning experiments and developed regression and least squares support vector machine (LS-SVM) models to predict the average surface roughness. Their models included five inputs: the tool nose radius, feed rate, depth of cut, discretization angle, and C-axis speed. They reported that the LS-SVM model provided better prediction capabilities than the regression model because the LS-SVM model had a better ability to model complex nonlinearities and interactions.

THE CONTRIBUTION OF THE PRESENT STUDY

The vast majority of existing research takes no account of the effect of the tool edge radius in the evaluation and modeling of machined surface roughness. One reason is that it has been challenging for tool manufacturers to ensure that the tool edge radius, typically at the level of micrometers, is uniformly distributed along a tool cutting edge, because of manufacturing errors. The tool edge radius measured at different locations along the same tool cutting edge can vary significantly from one location to another location.[1] Without cutting tools with a uniformly distributed tool edge radius along the same tool cutting edge, it is challenging for researchers to study the effect of the tool edge radius in machining. The vast majority of existing research seldom reports the magnitude of the tool edge radius employed in machining experiments.

The most significant contribution of the present study is that the effect of the tool edge radius is taken into account in the evaluation and modeling of machined surface roughness. Note that the tool edge radius[1] and tool nose radius[19] are two totally different concepts measured in different planes. Figure 1 shows the difference between the tool edge radius and tool nose radius. The tool nose radius is also called the tool corner radius and measured in the tool rake face. The magnitudes of the tool nose radius on commercial cutting tools are typically 0.2–1.2 mm. The tool edge radius is measured in the plane perpendicular to the tool cutting edge, and its magnitudes are often at the level of micrometers (μm). The effect of the tool nose radius on machined surface roughness has been well known and well documented in the literature.[19] However, there is little experimental study and theoretical modeling efforts on the effect of tool edge radius on machined surface roughness. The present study fills this important research gap.

FIG. 1

Difference between tool edge radius and tool nose radius.

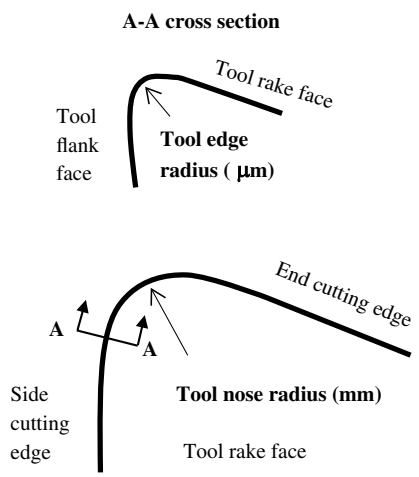

In addition, five surface roughness parameters, rather than the commonly used average surface roughness R_a only, were evaluated in the present study. A total of 45 cutting experiments were performed with tool inserts with three levels of tool edge radii and covered a range of cutting speed and feed rate conditions. The cutting tools employed in the present study were carefully selected from more than 20 commercially available triangular tool inserts involving more than 60 tool cutting edges. Each triangular tool insert had three tool cutting edges. Only those tool inserts with the most uniform distribution of tool edge radius along the same tool cutting edge were chosen in the present study. Based on the experimental data of cutting forces and vibrations, three types of models, including a multiple regression model, multilayer perceptron (MLP) neural network model, and radial basis function (RBF) neural network model, were developed to predict five surface roughness parameters.

In the remaining sections of this article, the experimental setup is described, including the work and tool materials, tool geometry, and cutting conditions. The measurements of the tool edge radius, machined surface roughness, cutting forces, and cutting vibrations are also described. The effect of the tool edge radius on the machined surface roughness, cutting forces, and cutting vibrations is presented and analyzed. The methods of multiple regression, MLP, and RBF neural network modeling are introduced, followed by a comparison of prediction accuracy using the three models. The major research findings are summarized at the end of the article.

Experimental Setup and Measurements

WORK MATERIAL

A computer-numerically-controlled turning center made by HAAS Automation Inc. (HAAS SL10) was employed to conduct three-dimensional (3-D) turning experiments on a UNS A92024-T351 aluminum alloy bar (ASTM B211, *Standard Specification for Aluminum and Aluminum-Alloy Rolled or Cold Finished Bar, Rod, and Wire*, grade). Aluminum alloys have been widely applied in a variety of industries, such as the aerospace and automotive industries.[20] UNS A92024-T351 aluminum alloy has the following chemical compositions in percentage of weight: aluminum: 90.7-94.7; chromium: 0.1 max; copper: 3.8-4.9; iron: 0.5 max; magnesium: 1.2 -1.8; manganese: 0.3-0.9; silicon: 0.5 max; titanium: 0.15 max; and zinc: 0.25 max.

TOOL MATERIAL AND GEOMETRY

The cutting tools used in machining experiments were three tool inserts of TPG432 made by Kennametal Inc. These triangular, flat-faced tool inserts were made of cemented carbides (Kennametal Carbide KC 8050) with titanium carbide/titanium nitride/titanium-carbon-nitride coating.

These tool inserts had the following common geometrical parameters: a tool working rake angle of 5°, tool working flank angle of 6°, tool working side cutting edge angle of 0°, and tool nose radius of 0.8 mm. However, the three tool inserts had different tool edge radii: 45.5 μm, 54.7 μm, and 72.4 μm. Note that the tool nose radius and tool edge radius are two different concepts because they are measured in different geometrical planes in 3-D space.[1]

Typically, tool manufacturers cannot accurately control the tool edge radius because of manufacturing errors. Therefore, the tool edge radius varies along the tool cutting edge on the same tool insert. The vast majority of existing research on machined surface roughness seldom reports the tool edge radius employed in its experimental work and modeling efforts. In the present study, the tool edge radius was carefully chosen after measuring more than 20 triangular tool inserts. Each triangular tool insert had three tool cutting edges. In other words, more than 60 tool cutting edges were measured. Only those tool inserts with the most uniform distribution of tool edge radius along the same tool cutting edge were chosen. They represented three levels of tool edge radii: 45.5 μm, 54.7 μm, and 72.4 μm. The measurement of the tool edge radius will be described in detail in a subsequent section.

CUTTING CONDITIONS

The cutting speed V varied at three levels: 150 m/min, 200 m/min, and 250 m/min. The feed rate f was chosen based on the tool edge radius r_ε and varied at five levels of f/r_ε ratios (r): 1.0, 1.5, 2.0, 2.5, and 3.0. The reason for

using f/r_ε ratios rather than f values alone is that the effect of tool edge radius in machining highly depends on the magnitude of the feed rate.[1] If the f/r_ε ratio is significantly large, say larger than ten, the cutting tool is typically considered a "sharp" tool, and the tool edge radius no longer plays a significant role in machining. Therefore, to magnify the effect of the tool edge radius, the ratio of f/r_ε was controlled to be no more than 3.0 in the present study.

Given three levels of cutting speeds (V), three levels of tool edge radii (r_ε), and five ratios (r) of feed rate to tool edge radius, a total of 45 ($3 \times 3 \times 5$) cutting experiments were conducted. In all the cutting experiments, the depth of cut was kept constant at 0.8 mm, the same as the tool nose radius. No cutting fluids were employed in order to facilitate the online and real-time measurements of cutting vibrations and forces.

Particularly worthy of mention is that all the cutting experiments were conducted with no substantial tool wear in order to avoid the effect of tool wear on machined surface roughness. Research has shown that tool wear has a significant effect on machined surface roughness.[21–24] For example, Jose et al.[21] studied the effect of tool wear and surface roughness in turning D2 steel. They reported that as tool wear increases machined surface roughness increases considerably. Liang and Liu[22] studied how tool wear affects machined surface topography in the machining of Ti-6Al-4V. They reported that when machined with the new sharp tool, the machined surface is relatively smooth. However, as the cutting process continues, tool wear develops on the tool flank face and has a profound effect on machined surface roughness.

To avoid the effect of tool wear on machined surface roughness, fresh cutting tools (rather than worn cutting tools) were employed in all the cutting experiments, and the cutting experiments were completed before noticeable tool wear was developed on either the tool rake face or flank face. The diameters of the aluminum workpiece varied between 62 mm and 87 mm. For an individual cutting experiment, the time of machining was less than ten seconds. Therefore, tool wear by secondary adhesion, a phenomenon commonly occurring in aluminum machining, was controlled and minimized in the present study.

OFF-LINE MEASUREMENTS OF TOOL EDGE RADIUS AND MACHINED SURFACE ROUGHNESS

Prior to the cutting experiments, the tool edge radius was measured off-line using a Mitutoyo-type SV602 measuring instrument, as shown in figure 2. The instrument had a diamond stylus with a tip radius of five μm. The tip radius of the diamond stylus was taken into account when measuring the tool edge radius and machined surface roughness. Measurements were taken at multiple locations along the same cutting edge to ensure that only those tool inserts with the most uniform distribution of tool edge radius along the tool cutting edge would be employed in the present study.

FIG. 2

Measurements of tool edge radius.

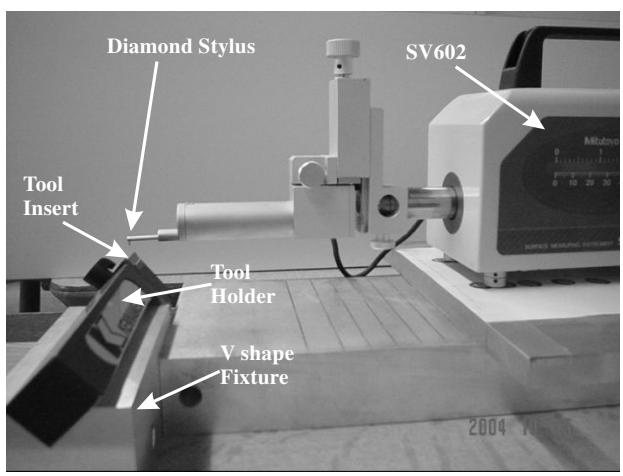

After the cutting experiments, the machined surface roughness was measured off-line, also using Mitutoyo-type SV602. The following five surface roughness parameters[25] were measured:

(1) Average roughness R_a: the arithmetic average of the absolute values of the roughness profile ordinates. R_a is the parameter most commonly used for evaluating the surface roughness.
(2) Root-mean-square (rms) roughness R_q: the rms average of the roughness profile ordinates.
(3) Peak roughness R_p: the maximum peak height of the roughness profile ordinates.
(4) Maximum roughness height R_{max}: the maximum peak-to-valley height of the roughness profile ordinates.
(5) Five-point average roughness R_z: the five-point average peak-to-valley height of the roughness profile ordinates.

It should be pointed out that the aforementioned surface roughness parameters were measured at three equally spaced locations around the circumference of the workpiece. The average values of the measurements at three locations were employed to represent the experimental values of machined surface roughness.

ONLINE REAL-TIME MEASUREMENTS OF CUTTING FORCES

For each cutting experiment, the cutting forces were measured online using a Kistler 9257B quartz three-component dynamometer, Kistler 5010B multichannel dual-mode charge amplifier, and LabVIEW, as shown in figure 3. The sampling rate was 10 kHz. MATLAB was employed to filter the high-frequency noise from the collected signals. The digital filter employed in MATLAB was Butterworth (1, 0.015). A MATLAB code was written to determine the average values of the three components of the cutting forces, namely the cutting force F_c, feed force F_f, and passive force F_p. These three forces were measured in the tangential (x- or the cutting speed), axial (y- or the feed rate), and radial (z- or the depth of cut) directions, respectively.

ONLINE REAL-TIME MEASUREMENTS OF CUTTING VIBRATIONS

The cutting vibrations were simultaneously measured online using a 356A63 Triaxial Integrated Circuit Piezoelectric (ICP) accelerometer that was fixed to the tool holder, as also shown in figure 3. The sensitivity of the accelerometer was 10 mV/g (±15 %), and its measurement range was ±5 g (peak). The accelerometer sensed the vibration signals in the x-, y-, and z-directions, i.e., the cutting speed, feed rate, and depth of cut directions, respectively.

FIG. 3 Measurements of cutting forces and vibrations.

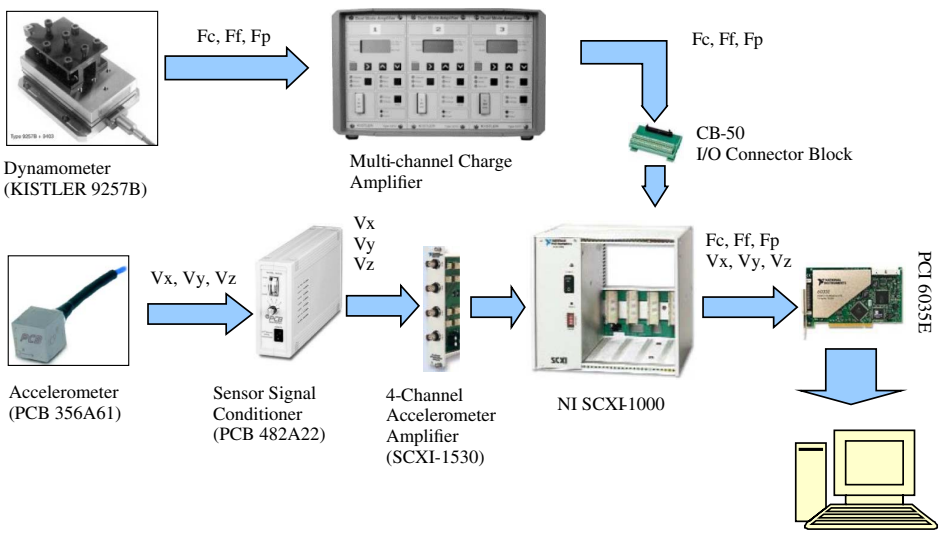

The sensed vibration signals, at the sampling frequency of 10 KHz, were sent to a PicoCoulomB (PCB) 482A22 low noise signal conditioner and a National Instruments (NI) SCXI-1530/1531 ICP accelerometer conditioning module. This amplified the conditioned signal, which was finally sent to a computer data acquisition system (LabVIEW) for further processing and signal display. The rms, which is the average of the squared values of the vibration amplitude, was calculated. The rms gives positive values that can be used for vibration analysis.

The Effect of Tool Edge Radius

Figures 4 and **5** show the effect of the tool edge radius on the machined surface roughness, cutting forces, and cutting vibrations under two representative experimental conditions, respectively—(1) the cutting speed of 250 m/min and feed rate to tool edge radius ratio of 2.0, and (2) the cutting speed of 350 m/min and feed rate to tool edge radius ratio of 2.5.

As seen clearly from **figures 4*A*** and **5*A***, all five surface roughness parameters increase as the tool edge radius increases. These varying trends can be explained based on the material flow and deformation in the tertiary deformation zone immediately beneath the tool cutting edge. In his analytical model of chip formation, Fang[1] has shown that the geometry and size of the tertiary deformation zone highly depends on the magnitude of the tool edge radius. As the tool edge radius increases, the tertiary deformation zone expands, which leads to more complex material flow and deformation within this zone as well as more complex elastic recovery of the deformed

FIG. 4 The effect of the tool edge radius on (*A*) machined surface roughness, (*B*) cutting forces, and (*C*) cutting vibrations at a cutting speed of 250 m/min and feed rate to tool edge radius ratio of 2.0.

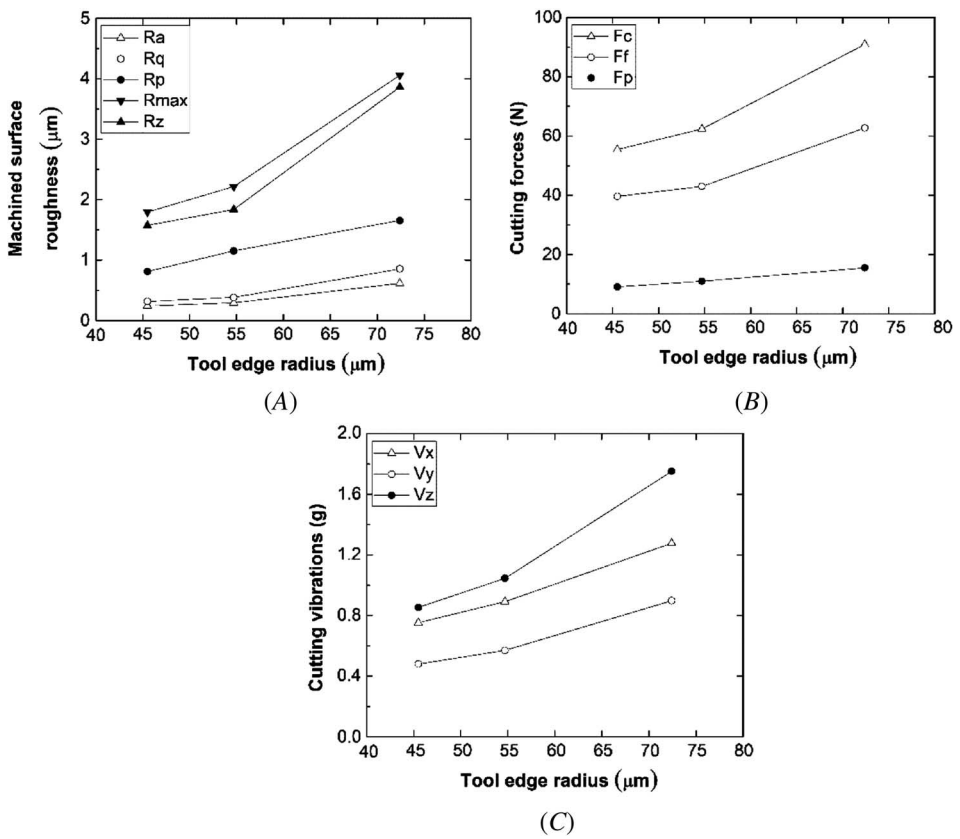

FIG. 5 The effect of the tool edge radius on (*A*) machined surface roughness, (*B*) cutting forces, and (*C*) cutting vibrations at a cutting speed of 350 m/min and feed rate to tool edge radius ratio of 2.5.

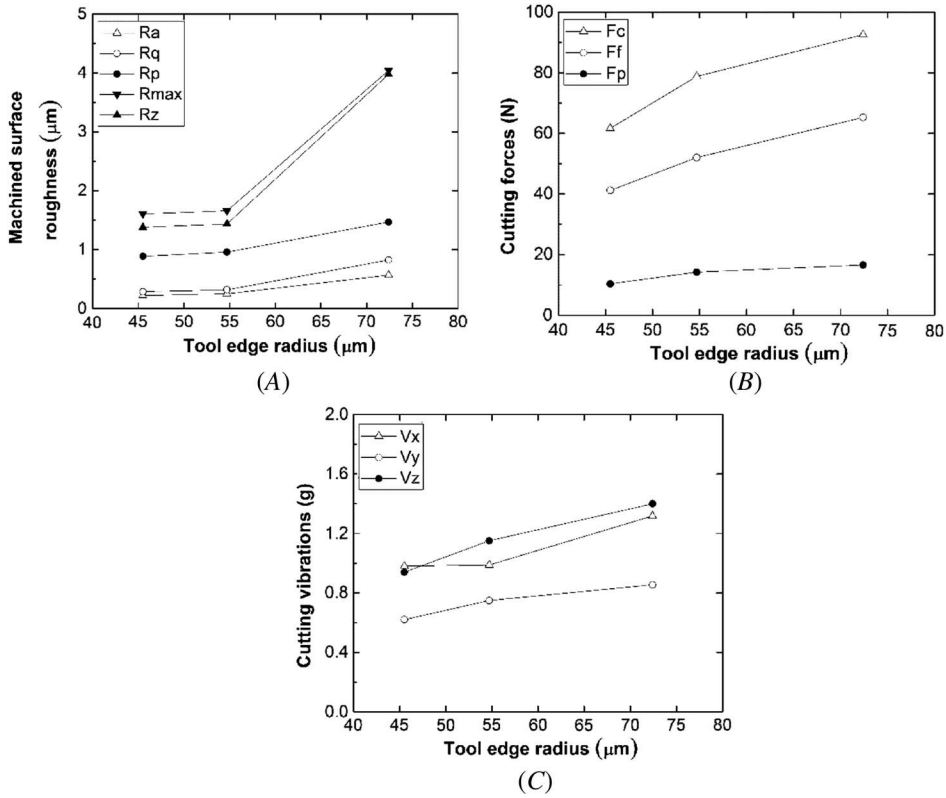

material immediately adjacent to the tertiary deformation zone. The complex elastic recovery of the deformed material contributes directly to the machined surface roughness.

Figures 4*B*, 5*B*, 4*C*, and 5*C* further show that all three components of cutting forces (F_c, F_f, and F_p) and cutting vibrations (V_x, V_y, and V_z) increase with an increase in the tool edge radius. These experimental results clearly demonstrate the effect of the tool edge radius on the cutting forces and vibrations. For both experimental conditions, the cutting force F_c and cutting vibration component V_z exhibit higher values when compared to other force and vibration components.

Multiple Regression Modeling

To explicitly and mathematically show how the machined surface roughness is affected by various factors, especially the tool edge radius, a multiple regression model was developed to predict the machined surface roughness. The multiple regression model has eight inputs: the tool edge radius r_ε, cutting speed V, feed rate to tool edge radius ratio r, three components of cutting forces (F_c, F_f, and F_p), and three components of cutting vibrations (V_x, V_y, and V_z). The outputs of the model are five surface roughness parameters: the average roughness R_a, rms roughness R_q, peak roughness R_p, maximum roughness height R_{max}, and five-point average roughness R_z.

Among 45 cutting experiments, the datasets for 38 experiments (representing 85 % of all the data collected) were randomly selected as training data to establish the multiple regression model. The data set for the remaining seven experiments (representing 15 % of all the data collected) was employed as test data to validate the prediction

accuracy of the model. Interactions among inputs (or called predictor variables) were found to be of no statistical significance. The following equations (1)–(5) show the multiple regression model developed in the present study, considering the individual parameters:

$$R_a = 0.6041 r_\varepsilon^{\mathbf{5.26}} V^{0.000477} r^{0.0367} F_c^{0.00041} F_f^{0.01433} F_p^{-0.0263} V_x^{-0.240} V_y^{0.2043} V_z^{0.0171} \quad (1)$$

$$R_q = 0.479 r_\varepsilon^{\mathbf{7.64}} V^{0.000555} r^{0.0504} F_c^{0.00221} F_f^{0.01852} F_p^{-0.0365} V_x^{-0.272} V_y^{0.298} V_z^{-0.044} \quad (2)$$

$$R_p = 0.2516 r_\varepsilon^{\mathbf{15.40}} V^{0.002534} r^{0.201} F_c^{0.0144} F_f^{0.0095} F_p^{-0.0727} V_x^{-0.620} V_y^{0.385} V_z^{0.154} \quad (3)$$

$$R_{max} = 0.0517 r_\varepsilon^{\mathbf{28.8}} V^{0.00378} r^{0.097} F_c^{-0.0075} F_f^{0.0887} F_p^{-0.080} V_x^{-1.305} V_y^{1.269} V_z^{-0.005} \quad (4)$$

$$R_z = 0.0485 r_\varepsilon^{\mathbf{26.4}} V^{0.00361} r^{0.093} F_c^{-0.0102} F_f^{0.0892} F_p^{-0.055} V_x^{-1.361} V_y^{1.385} V_z^{-0.085} \quad (5)$$

The effect of the tool edge radius on the machined surface roughness is highlighted in the bold letters and digits in these five equations. To determine how well the aforementioned model fits the data, *R*-squared (R^2) values were calculated. In general, the higher the *R*-squared value, the better the model fits the data. The results show that the *R*-squared values are 0.859 for average roughness R_a, 0.8645 for rms roughness R_q, 0.8225 for peak roughness R_p, 0.8503 for maximum roughness height R_{max}, and 0.8471 for five-point average roughness R_z. These results mean that the nine predictor variables included in the multiple regression model account for 85.9 %, 86.45 %, 82.25 %, 85.03 %, and 84.71 % of the variations in R_a, R_q, R_p, R_{max}, and R_z, respectively.

Refer to the positive or negative exponents in equations (1)–(5). For all five surface roughness parameters (R_a, R_q, R_p, R_{max}, and R_z), the exponents for the tool edge radius r_ε, cutting speed V, feed rate to tool edge radius ratio r, feed force F_f, and cutting vibration in the feed rate direction V_y, are positive. The exponents for the cutting force F_c, cutting vibration in the cutting speed direction V_x, and cutting vibration in depth of cut direction V_z are not always positive. These observations imply that, in general, the machined surface roughness increases with the increasing tool edge radius r_ε, cutting speed V, feed rate to tool edge radius r, feed force F_f, and cutting vibrations in the feed rate direction V_y.

Neural Network Modeling

Two types of neural network models—an MLP model and RBF model—were further developed to compare their prediction accuracy with the multiple regression model. Both the neural network models have the same inputs and outputs as the multiple regression model. The data employed to train and test both the neural network models were also the same as those described in the previous section.

MLP NEURAL NETWORK MODEL

Based on back-propagation, MLP neural networks are one of the most popular networks employed in the engineering field, including machining.[26–28] The MLP model does not have simple and explicit mathematical forms to present in this article. Instead, the MATLAB computer software package[29] was employed to develop computer codes for the MLP model. The number of neurons in the hidden layer varied in order to develop a model that generalized well. The activation function used in the hidden neurons was *logsig*. In this paper, MATLAB functions are highlighted in italics. The output neuron had a linear activation function.

Two standard built-in functions within MATLAB—*trainrp* and *traingdm*—were initially selected to train the MLP model. **Table 1** shows the results of a comparison between the two training algorithms, including the number of hidden neurons for each training algorithm for two representative surface roughness parameters, R_a and R_{max}. The mean squared error (MSE) for training was 0.01. From **Table 1**, the *trainrp* algorithm is much more efficient than *traingdm* for R_a and R_{max}, because *trainrp* takes a smaller number of epochs (within 20) to reach the set error levels. However, it requires as many as 7,507 epochs (depending on the number of hidden neurons) for

TABLE 1
Comparison between the *trainrp* and *traingdm* algorithms

Surface Roughness Parameters	Number of Hidden Neurons	*trainrp* Algorithm: Number of Epochs	*Trainrp* Algorithm: Error Reached	*Traingdm* Algorithm: Number of Epochs for Target Error 0.01
Average roughness R_a	8	8	0.00799	7,507
	10	5	0.00986	3,131
	12	10	0.00903	2,838
	14	6	0.00864	2,977
	16	10	0.00887	2,183
Maximum roughness	8	6	0.00966	3,810
height R_{max}	10	8	0.00794	3,915
	12	6	0.00919	3,723
	14	10	0.00974	3,470
	16	8	0.00893	1,462

the *traingdm* algorithm to reach the same error level. Therefore, the *trainrp* algorithm was employed to train the MLP model for R_a and R_{max}. The number of hidden neurons selected was based on the generalization capacity of the network in terms of its classification performance on the data.

Table 2 summarizes the accuracy of the best MLP model for predicting the five surface roughness parameters based on the training and test data. The accuracy (in percentage) in Table 2 is defined as (fitted or predicted value – measured value) / measured value. The second column in Table 2 also shows the optimal architecture of the best MLP model for each surface roughness parameter. For example, the optimal architecture of the best MLP model for R_a is 9-8-1 (*trainrp*), which means the model contains 9 inputs, 8 hidden neurons, and 1 output, and the best MLP model uses the *trainrp* algorithm. The optimal architecture of the best MLP model for R_z is 9-10-1 (*traingdm*), which means the model contains 9 inputs, 10 hidden neurons, and 1 output, and the best MLP model uses the *traingdm* algorithm.

RBF NEURAL NETWORKS

RBF neural networks are a different class of neural network models that have not been widely applied in the evaluation and modeling of machined surface roughness. In addition to the input and output layers, the RBF model includes a hidden layer with a nonlinear RBF activation function. In the RBF algorithm, a method called curve fitting in a high dimensional space is employed, which involves the process of finding a surface in a multidimensional space to provide a best fit to the training data. A detailed description of the RBF algorithm can be found in relevant literature.[30]

In the present study, MATLAB was also employed to develop the computer code for an RBF neural network model. The function used for design was *newrb*.[29] One of the important parameters for training using this function is the spread (width) of RBF functions. The spread (width) selection was made based on the performance of the network on the training and test data.

TABLE 2
The accuracy of the best MLP model for predicting five surface roughness parameters

Surface Roughness Parameter	The Best MLP Model	Accuracy Based on Training Data, %	Accuracy Based on Test Data, %
R_a	9-8-1 (*trainrp*)	100	71.42
R_q	9-10-1 (*trainrp*)	92.1	85.71
R_p	9-16-1 (*traingdm*)	81.57	71.42
R_{max}	9-14-1 (*trainrp*)	86.84	85.71
R_z	9-10-1 (*traingdm*)	86.84	85.71

TABLE 3
The performance of the RBF neural networks for different values of the RBF spread (width)

Surface Roughness Parameters	Spread (Width)	Optimal Number of RBF Hidden Units	Epochs	Accuracy Based on Training Data, %	Accuracy Based on Test Data, %
Average roughness R_a	0.1	16	33	97.36	71.42
	0.2	16	33	97.36	71.42
	0.3	16	33	97.36	71.42
	0.4	16	33	97.36	71.42
Maximum roughness height R_{max}	0.1	8	123	34.21	14.28
	0.2	8	123	34.21	14.28
	0.3	8	123	34.21	14.28
	0.4	8	123	34.21	14.28

Using two representative surface roughness parameters R_a and R_{max} as examples, Table 3 summarizes the performance of RBF neural networks for different values of RBF spread (width). The accuracy (in percentage) in Table 3 is also defined as (fitted or predicted value – measured value) / measured value. The third column in Table 3 also lists the optimal number of RBF hidden units selected based on the optimal network performance. As seen clearly from Table 3, the accuracy of the RBF model is not affected by the RBF spread (width) for both the training and test data in the present study. The accuracy of the RBF model is higher for R_a than R_{max}.

Comparison Among Three Types of Models

The prediction accuracy is compared among the multiple regression model, MLP neural network model, and RBF neural network model. All three models have the same sets of inputs and outputs. The same training data were also employed to develop these three models.

Figure 6 shows the comparison of the three models based on the training data, using two representative surface roughness parameters R_a and R_{max} as examples. Figure 7 shows the comparison of the three models based on the test data for all five surface roughness parameters. Based on the results shown in figure 7, the average MSE were further calculated to quantitatively compare the prediction accuracy of the three models. The MSE is a statistical term measuring the difference between the estimator and what is measured.[31] It is calculated as follows:[31]

FIG. 6 A comparison of the three models based on the training data for two representative examples: (*A*) average roughness R_a and (*B*) maximum roughness height R_{max}.

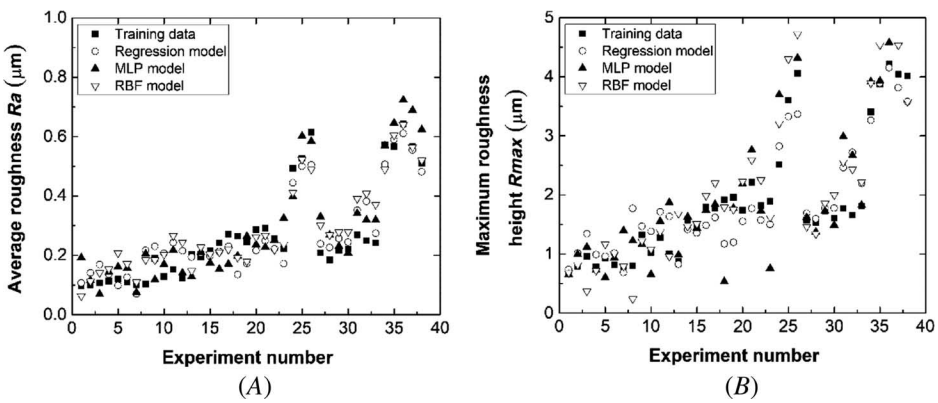

FIG. 7 A comparison of the three models based on the test data for (*A*) average roughness R_a, (*B*) rms roughness R_q, (*C*) peak roughness R_p, (*D*) maximum roughness height R_{max}, and (*E*) five-point average roughness R_z.

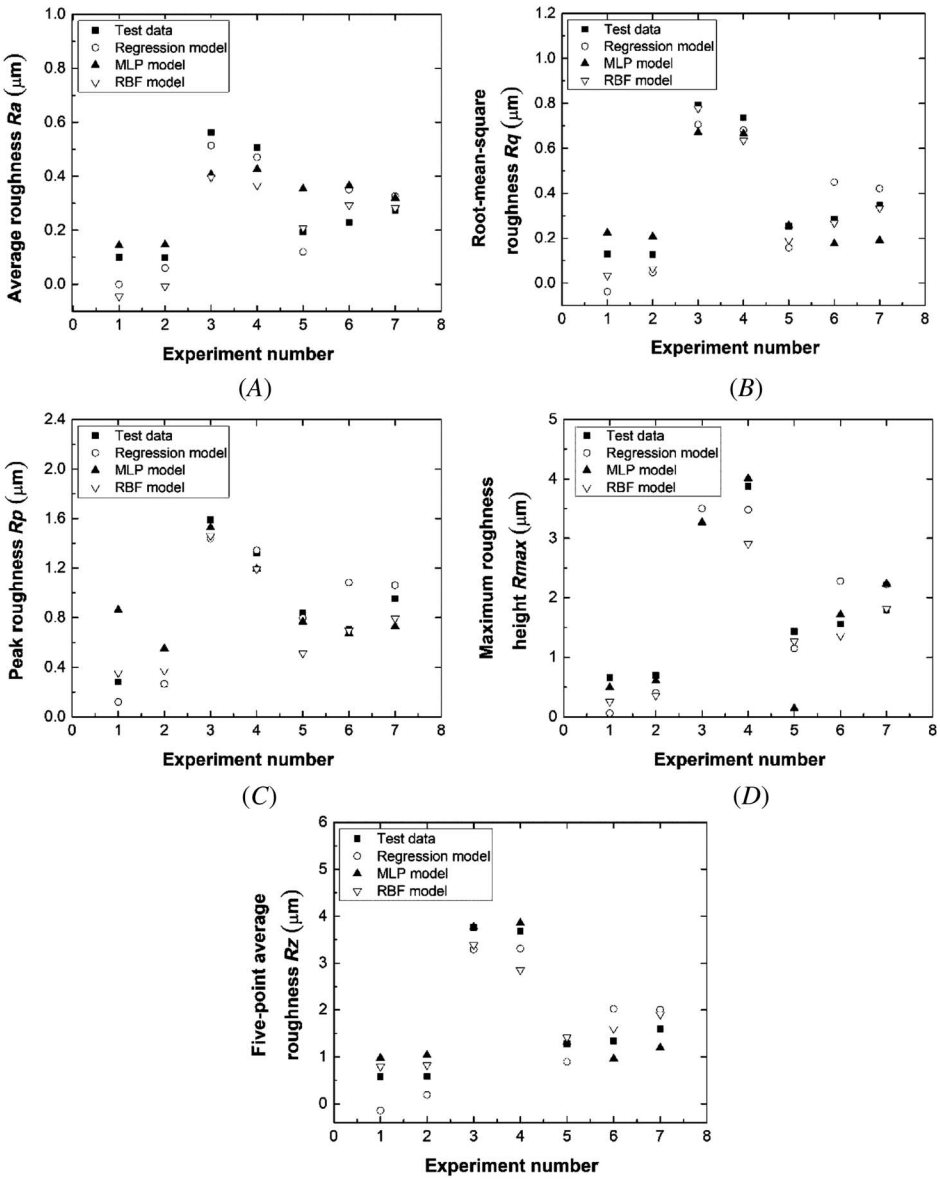

$$\text{MSE} = \frac{1}{n}\sum_{i=1}^{n}(\text{measured value } i - \text{predicted value } i)^2 \tag{6}$$

The lower the MSE value, the higher prediction accuracy the model has. **Table 4** shows a comparison of the average MSE among the three models for the five surface roughness parameters. It can be seen clearly from **Table 4** that different models lead to different prediction accuracies for different surface roughness parameters. In the terms of average MSE, the multiple regression model has the highest accuracy (0.2743 %) for predicting the average roughness R_a. The MLP neural network model has the highest accuracy (5.04 %) for predicting the

TABLE 4
Comparison of the average MSE among the three models based on the test data

	Average MSE %				
Predictive Models	Average Roughness R_a	rms Roughness R_q	Peak Roughness R_p	Maximum Roughness Height R_{max}	Five-Point Average Roughness R_z
Multiple regression model	0.2743	0.6210	1.4713	11.2370	12.9216
MLP neural network model	0.5813	0.5114	3.5524	17.0511	5.0413
RBF neural network model	0.5990	0.1976	1.2902	9.3819	8.0130

five-point average roughness R_z. The RBF neural network model has the highest accuracy (0.1967 %, 1.2902 %, and 9.3819 %) for predicting the rms roughness R_q, peak roughness R_p, and maximum roughness height R_{max}, respectively. The prediction accuracy is less than 4 % for R_a, R_q, and R_p for all three models.

Conclusions

The tool edge radius plays a significant role in machining and is an important factor to consider in precision and ultraprecision machining. However, in the evaluation and modeling of machined surface roughness, the vast majority of existing research takes no account of the effect of the tool edge radius. The present study has filled this critical research gap by conducting a total of 45 cutting experiments that involved three levels of tool edge radii. The cutting tools employed in the present study were carefully chosen from more than 20 commercial tool inserts based on the multiple measurements of tool edge radius along the same tool cutting edge.

The experimental results from the present study have shown that the tool edge radius has a profound effect on the machined surface roughness, cutting forces, and cutting vibrations. An increase in the tool edge radius results in increases in all five surface roughness parameters, including average roughness R_a, rms roughness R_q, peak roughness R_p, maximum roughness height R_{max}, and five-point average roughness R_z.

Three types of models have also been developed from the present study, including a multiple regression model, MLP neural network model, and RBF neural network model. Based on the average MSE, the multiple regression model has the highest accuracy, 0.2743 %, for predicting the average roughness R_a. The MLP neural network model outperforms the other two models in predicting the five-point average roughness R_z, with the highest prediction accuracy of 5.04 %. The RBF neural network model outperforms the other two models in predicting the rms roughness R_q, peak roughness R_p, and maximum roughness height R_{max}, with prediction accuracy of 0.1967 %, 1.2902 %, and 9.3819 %, respectively.

References

1. N. Fang, "Slip-Line Modeling of Machining with a Rounded-Edge Tool—Part I: New Model and Theory," *Journal of the Mechanics and Physics of Solids* 51, no. 4 (April 2003): 715–742, https://doi.org/10.1016/s0022-5096(02)00060-1
2. Y. Karpat, "Investigation of the Effect of Cutting Tool Edge Radius on Material Separation Due to Ductile Fracture in Machining," *International Journal of Mechanical Sciences* 51, no. 7 (July 2009): 541–546, https://doi.org/10.1016/j.ijmecsci.2009.05.005
3. R. J. Schimmel, W. J. Endres, and R. Stevenson, "Application of an Internally Consistent Material Model to Determine the Effect of Tool Edge Geometry in Orthogonal Machining," *Journal of Manufacturing Science and Engineering* 124, no. 3 (July 2002): 536–543, https://doi.org/10.1115/1.1448334
4. P. Huang and W. B. Lee, "Cutting Force Prediction for Ultra-Precision Diamond Turning by Considering the Effect of Tool Edge Radius," *International Journal of Machine Tools and Manufacture* 109 (October 2016): 1–7, https://doi.org/10.1016/j.ijmachtools.2016.06.005
5. M. Arif, M. Rahman, and W. Y. San, "A Study on the Effect of Tool-Edge Radius on Critical Machining Characteristics in Ultra-Precision Milling of Tungsten Carbide," *International Journal of Advanced Manufacturing Technology* 67, nos. 5–8 (July 2013): 1257–1265, https://doi.org/10.1007/s00170-012-4563-8

6. I. S. Kang, J. S. Kim, and Y. W. Seo, "Cutting Force Model Considering Tool Edge Geometry for Micro End Milling Process," *Journal of Mechanical Science and Technology* 22, no. 2 (February 2008): 293–299, https://doi.org/10.1007/s12206-007-1110-x
7. K. Yang, Y.-C. Liang, K.-N. Zheng, Q.-S. Bai, and W.-Q. Chen, "Tool Edge Radius Effect on Cutting Temperature in Micro-End-Milling Process," *International Journal of Advanced Manufacturing Technology* 52, nos. 9–12 (February 2011): 905–912, https://doi.org/10.1007/s00170-010-2795-z
8. W. J. Endres and R. K. Kountanya, "The Effects of Corner Radius and Edge Radius on Tool Flank Wear," *Journal of Manufacturing Processes* 4, no. 2 (July 2002): 89–96, https://doi.org/10.1016/s1526-6125(02)70135-7
9. M. N. A. Nasr, E.-G. Ng, and M. A. Elbestawi, "Modelling the Effects of Tool-Edge Radius on Residual Stresses When Orthogonal Cutting AISI 316L," *International Journal of Machine Tools and Manufacture* 47, no. 2 (February 2007): 401–411, https://doi.org/10.1016/j.ijmachtools.2006.03.004
10. S. J. Zhang, S. To, S. J. Wang, and Z. W. Zhu, "A Review of Surface Roughness Generation in Ultra-Precision Machining," *International Journal of Machine Tools and Manufacture* 91 (April 2015): 76–95, https://doi.org/10.1016/j.ijmachtools.2015.02.001
11. J. Kopač, M. Bahor, and M. Soković, "Optimal Machining Parameters for Achieving the Desired Surface Roughness in Fine Turning of Cold Pre-formed Steel Workpieces," *International Journal of Machine Tools and Manufacture* 42, no. 6 (May 2002): 707–716, https://doi.org/10.1016/s0890-6955(01)00163-8
12. A. K. Ghani, I. A. Choudhury, and Husni, "Study of Tool Life, Surface Roughness and Vibration in Machining Nodular Cast Iron with Ceramic Tool," *Journal of Materials Processing Technology* 127, no. 1 (September 2002): 17–22, https://doi.org/10.1016/s0924-0136(02)00092-4
13. K. A. Risbood, U. S. Dixit, and A. D. Sahasrabudhe, "Prediction of Surface Roughness and Dimensional Deviation by Measuring Cutting Forces and Vibrations in Turning Process," *Journal of Materials Processing Technology* 132, nos. 1–3 (January 2003): 203–214, https://doi.org/10.1016/s0924-0136(02)00920-2
14. J. Grum and M. Kisin, "Influence of Microstructure on Surface Integrity in Turning—Part I: The Influence of the Size of the Soft Phase in a Microstructure on Surface-Roughness Formation," *International Journal of Machine Tools and Manufacture* 43, no. 15 (December 2003): 1535–1543, https://doi.org/10.1016/s0890-6955(03)00199-8
15. I. Scandiffio, A. E. Diniz, and A. F. de Souza, "Evaluating Surface Roughness, Tool Life, and Machining Force when Milling Free-Form Shapes on Hardened AISI D6 Steel," *International Journal of Advanced Manufacturing Technology* 82, nos. 9–12 (February 2016): 2075–2086, https://doi.org/10.1007/s00170-015-7525-0
16. R. Jahn and H. Truckenbrodt, "A Simple Fractal Analysis Method of the Surface Roughness," *Journal of Materials Processing Technology* 145, no. 1 (January 2004): 40–45, https://doi.org/10.1016/s0924-0136(03)00860-4
17. W. Grzesik and S. Brol, "Hybrid Approach to Surface Roughness Evaluation in Multistage Machining Processes," *Journal of Materials Processing Technology* 134, no. 2 (March 2003): 265–272, https://doi.org/10.1016/s0924-0136(02)01105-6
18. I. Maher, M. E. H. Eltaib, A. A. D. Sarhan, and R. M. El-Zahry, "Cutting Force-Based Adaptive Neuro-Fuzzy Approach for Accurate Surface Roughness Prediction in End Milling Operation for Intelligent Machining," *International Journal of Advanced Manufacturing Technology* 76, nos. 5–8 (February 2015): 1459–1467, https://doi.org/10.1007/s00170-014-6379-1
19. X. S. Wang, M. Kang, X.-Q. Fu, and C.-L. Li, "Predictive Modeling of Surface Roughness in Lenses Precision Turning Using Regression and Support Vector Machines," *International Journal of Advanced Manufacturing Technology* 87, nos. 5–8 (November 2016): 1273–1281, https://doi.org/10.1007/s00170-013-5231-3
20. H. Fukui, J. Okida, N. Omori, H. Moriguchi, and K. Tsuda, "Cutting Performance of DLC Coated Tools in Dry Machining Aluminum Alloys," *Surface and Coatings Technology* 187, no. 1 (October 2004): 70–76, https://doi.org/10.1016/j.surfcoat.2004.01.014
21. B. Jose, K. Nikita, T. Patil, S. Hemakumar, and P. Kuppan, "Online Monitoring of Tool Wear and Surface Roughness by Using Acoustic and Force Sensors," *Materials Today: Proceedings* 5, no. 2, part 2 (2018): 8299–8306, https://doi.org/10.1016/j.matpr.2017.11.521
22. X. Liang and Z. Liu, "Tool Wear Behaviors and Corresponding Machined Surface Topography during High-Speed Machining of Ti-6Al-4V with Fine Grain Tools," *Tribology International* 121 (May 2018): 321–332, https://doi.org/10.1016/j.triboint.2018.01.057
23. S. A. Ashrafi, A. Davoudinejad, and A. Niazi, "Investigations into Effect of Tool Wear on Surface Integrity in Dry Turning of Al6061," *Advanced Materials Research* 622–623 (December 2012): 375–379, https://doi.org/10.4028/www.scientific.net/amr.622-623.375
24. F. A. Niaki and L. Mears, "A Comprehensive Study on the Effects of Tool Wear on Surface Roughness, Dimensional Integrity and Residual Stress in Turning IN718 Hard-to-Machine Alloy," *Journal of Manufacturing Processes* 30 (December 2017): 268–280, https://doi.org/10.1016/j.jmapro.2017.09.016
25. D. Whitehouse, *Surfaces and Their Measurement* (Oxford, UK: Butterworth-Heinemann, 2002).
26. J. L. Rosa, ed., *Artificial Neural Networks—Models and Applications* (London: IntechOpen, 2016).
27. M. T. Hagan, H. B. Demuth, M. H. Beale, and O. D. Jesús, *Neural Network Design*, 2nd ed. (Stillwater: Martin Hagan, 2014).
28. T. Masters, *Signal and Image Processing with Neural Networks* (Hoboken, NJ: John Wiley & Sons, 1994).
29. M. H. Beale, M. T. Hagan, and H. B. Demuth, *Neural Network Toolbox User's Guide* (Natick, MA: The MathWorks Inc., 2015).
30. S. Haykin, *Neural Networks: A Comprehensive Foundation*, 2nd ed. (Upper Saddle River, NJ: Prentice Hall, 1998).
31. E. L. Lehmann and G. Casella, *Theory of Point Estimation*, 2nd ed. (New York: Springer, 1998).